

# Synthesis and Characterization of Hypercoordinated Silicon Anions: Catching Intermediates of Lewis Base Catalysis

Nils Ansmann<sup>+</sup>, Deborah Hartmann<sup>+</sup>, Sonja Sailer, Philipp Erdmann, Rezisha Maskey, Marcel Schorpp, and Lutz Greb\*

**Abstract:** Anionic hypercoordinated silicates with weak donors were proposed as key intermediates in numerous silicon-based reactions. However, their short-lived nature rendered even spectroscopic observations highly challenging. Here, we characterize hypercoordinated silicon anions, including the first bromido-, iodido-, formato-, acetato-, triflato- and sulfato-silicates. This is enabled by a new, donor-free polymeric form of Lewis superacidic bis(perchlorocatecholato)silane **1**. Spectroscopic, structural, and computational insights allow a reassessment of Gutmann's empirical rules for the role of silicon hypercoordination in synthesis and catalysis. The electronic perturbations of **1** exerted on the bound anions indicate pronounced substrate activation.

## Introduction

Compounds with penta- or hexacoordinated silicon atoms exhibit structures and reactivities markedly enhanced compared to their tetracoordinated counterparts.<sup>[1]</sup> Consequently, tetravalent silicon-based reagents can be activated by adding external donors,<sup>[2]</sup> constituting the field of n- $\sigma^*$ -type Lewis base catalysis.<sup>[3]</sup> Based on empirical analyses, Gutmann proposed two rules that are operative during Lewis base activation (Figure 1a):<sup>[4]</sup> 1) Binding a donor to silicon causes a bond elongation to the remaining ligands and increases their nucleophilicity. The shorter the bond to the added donor, the stronger this bond elongation. 2)

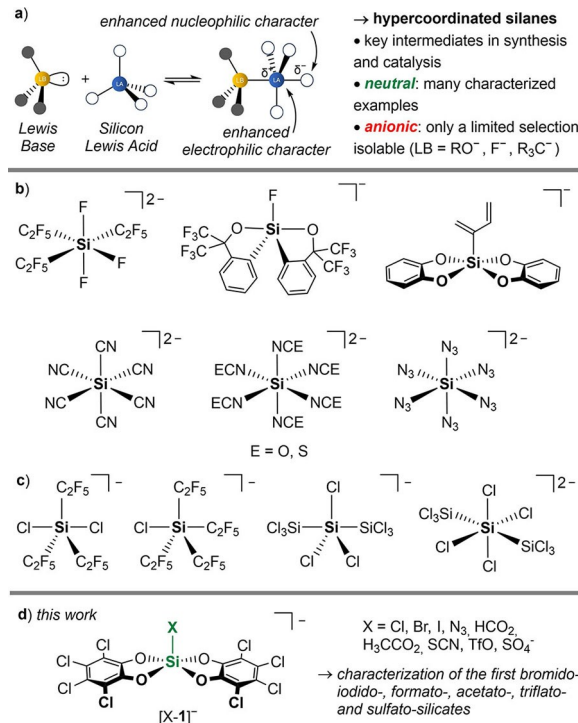


**Figure 1.** a) Gutmann's assumptions on the role of hypercoordinated silanes in Lewis base catalysis. b) Examples for isolable hypercoordinated silicate anions with strong donors and *pseudo-halides*. c) Chlorido-silicates as the recent addendums to hypercoordinated silicate anions, d) Bis(perchlorocatecholato) silane-derived hypercoordinated silicate anions  $[X-1]^-$  described in this work.

Binding a donor to silicon enhances the positive polarization at silicon and thus also its electrophilicity. Whereas initial studies relied on strong neutral (e.g., phosphoramides) or anionic donors (e.g., fluoride), weak bases were also found successful.<sup>[5]</sup> Hence, weak adducts such as acetato- or bromido-silicates were proposed as key intermediates in, e.g., aldol or cyanosilylation reactions but never confirmed spectroscopically.<sup>[6]</sup> Hypercoordinated silicate anions were also suggested as active species in numerous other transformations, but their fleeting nature demanded sophisticated tools for mechanistic conclusions.<sup>[7]</sup> Indeed, whereas many *neutral* hypercoordinated silanes have been characterized, much less is known about the *anionic* counterparts.<sup>[1]</sup> This instability originates from silicon's moderate Lewis acidity, the high charge density in complexes of this relatively small central element, and the pronounced solvation free energy

[\*] Prof. Dr. L. Greb

Department of Chemistry and Biochemistry-Inorganic Chemistry  
Freie Universität Berlin  
Fabeckstr. 34/36, 14195 Berlin (Germany)  
E-mail: lutz.greb@fu-berlin.de

N. Ansmann,<sup>+</sup> Dr. D. Hartmann,<sup>+</sup> S. Sailer, P. Erdmann, R. Maskey, Dr. M. Schorpp  
Anorganisch-Chemisches Institut  
Ruprecht-Karls-Universität Heidelberg  
Im Neuenheimer Feld 270, 69120 Heidelberg (Germany)

[+] These authors contributed equally to this work.

© 2022 The Authors. Angewandte Chemie International Edition published by Wiley-VCH GmbH. This is an open access article under the terms of the Creative Commons Attribution Non-Commercial License, which permits use, distribution and reproduction in any medium, provided the original work is properly cited and is not used for commercial purposes.

of dissociated anionic ligands.<sup>[8]</sup> Hypercoordinated silicon anions have been isolated only with donors of high silicon affinities such as alkoxide, fluoride, or inert carbanionic groups (Figure 1b for some examples).<sup>[9]</sup> A remarkable extension transpired from research on complexes of the linear cyanido-,<sup>[10]</sup> (thio)cyanato-,<sup>[11]</sup> azido-,<sup>[12]</sup> or related donors (Figure 1b).<sup>[13]</sup> Noteworthily, species as fundamental as anionic chlorido-silicates were described only recently (Figure 1c).<sup>[14]</sup>

In the present work, we characterize the first anionic bromido-, iodido-, formato-, acetato-, triflato- and sulfato-silicates  $[X\text{-}\mathbf{1}]^-$  (Figure 1d). The required silicon-centered affinity is provided by a “donor-free” form of bis(perchlorocatecholato)silane **1**, whose bis-acetonitrile adduct was introduced as a neutral silicon-based Lewis superacid recently.<sup>[15]</sup> By that, critical intermediates of Lewis base catalysis are tracked, providing insights on the degree of structural and electronic perturbation of the silicon reagents upon anion binding.

## Results and Discussion

We launched our studies by computing various ion affinities (enthalpies) of **1** at the highly accurate, isodesmic DLPNO-CCSD(T)/aug-cc-pVQZ//PBEh-3c/def2-mSVP level of theory in the gas phase and solvation corrected (COSMO-RS,  $\text{CH}_2\text{Cl}_2$ ; see Table 1, for the  $\text{Me}_3\text{Si}^+$ -isodesmic scheme with CCSD(T)/CBS anchor values, see section 3 in the Supporting Information). A bridging binding mode of the anions, as found in  $[\text{Me}_3\text{Si-X-SiMe}_3][\text{B}(\text{C}_6\text{F}_5)_4]$  ( $\text{X}=\text{F}, \text{Cl}, \text{Br}, \text{I}, \text{CN}, \text{OCN}, \text{SCN}, \text{N}_3$ )<sup>[16]</sup> was not considered, except for the sulfate dianion. All adduct formations of  $[X\text{-}\mathbf{1}]^-$  were predicted sufficiently exothermic, both in the gas and solution phase. For the ambidentate isothiocyanate ion, the *N*-bound adduct  $[\text{SCN-}\mathbf{1}]^-$  was found to be more stable by  $-70.4 \text{ kJ mol}^{-1}$ . Apart from the fluoride ion, the highest affinities in solution were computed toward acetate and formate, whereas the lowest affinity was found for iodide. Remarkably, the solution affinity of **1** is up to  $100 \text{ kJ mol}^{-1}$

**Table 1:** Computed X-ion affinities (DLPNO-CCSD(T)/ aug-cc-pVQZ//PBEh-3c/def2-mSVP) of **1**.

$[\text{X-}\mathbf{1}]^-$	X-ion affinity $[\text{kJ mol}^{-1}]$	X-ion affinity (COSMO-RS) $[\text{kJ mol}^{-1}]$
F	-507.1	-314.5
Cl	-293.8	-149.3
Br	-262.6	-109.1
I	-196.0	-62.2
$\text{N}_3$	-304.1	-154.9
$\kappa^1\text{-HCOO}$	-327.3	-177.8
$\kappa^2\text{-HCO}_2$	-322.5	-178.2
$\kappa^1\text{-H}_3\text{CCOO}$	-316.4	-173.2
$\kappa^2\text{-H}_3\text{CCO}_2$	-330.7	-198.8
SCN	-191.9	-68.8
NCS	-262.3	-135.0
$\kappa^1\text{-TfO}$	-245.7	-129.3
$\kappa^2\text{-TfO}$	-220.9	-110.0
$[\mathbf{1}-\text{SO}_4\text{-}\mathbf{1}]^{2-}$	-713.2	-163.3

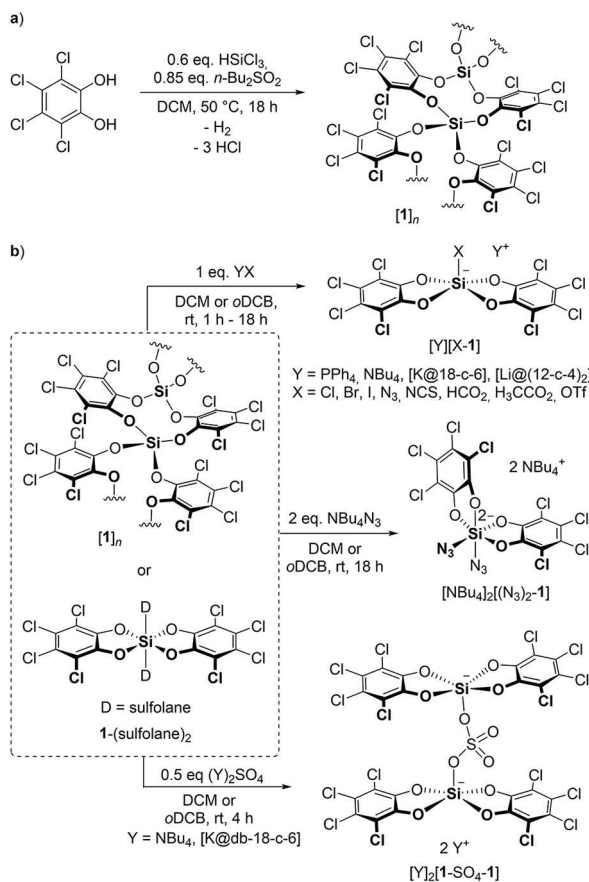
larger than for  $\text{SiCl}_4$  or even up to  $200 \text{ kJ mol}^{-1}$  compared to  $\text{Si}(\text{OMe})_4$ , rendering respective adduct formation with conventional silanes as unlikely (see section 3c in the Supporting Information).

Thus, we turned our attention to the synthetic realization. It should be noted that this study aimed for the analysis of adduct formation by NMR spectroscopy and single-crystal X-ray diffraction,<sup>[17]</sup> whereas the isolation of the bulk products was not attempted. A proper choice of the Lewis acid starting material proved critical for a successful reaction. The originally introduced acetonitrile bisadduct **1**-(MeCN)<sub>2</sub> caused side reactions with several salts of the anionic donor. Hence, a precursor of **1** with a chemically more robust but sufficiently labile donor had to be devised. The bisadduct of **1** with sulfolane ( $\text{C}_4\text{H}_8\text{SO}_2$ ), a donor of strength similar to acetonitrile but with a diminished propensity for electrophilic reactions, was prepared.<sup>[18]</sup> Indeed, upon mixing **1**-(sulfolane)<sub>2</sub> with the corresponding salts, successful formation of the desired compounds  $[X\text{-}\mathbf{1}]^-$  were observed by multinuclear NMR spectroscopy (see below for discussion). Still, sulfolane’s high boiling point and poor solubility rendered its subsequent removal difficult, while crystallization attempts of the sulfolane-containing mixtures led to the crystallization of **1**-(sulfolane)<sub>2</sub>. Hence, a donor-free precursor of **1** was needed for crystallographic evidence. According to our previous studies on the structure of bis(catecholato)silanes,<sup>[19]</sup> it was assumed that donor-free **1** would adopt a polymeric structure  $[\mathbf{1}]_n$  (Scheme 1a).

Indeed, the synthesis of  $[\mathbf{1}]_n$  was achieved by adding substoichiometric amounts of *n*-butylsulfone (0.85 equiv) to  $\text{HSiCl}_3$  and perchlorocatechol in DCM. This donor is sufficiently nucleophilic to initiate the  $\text{H}_2/\text{HCl}$  release and Si–O bond formation, but weak enough to escape the final product upon liquid-phase extraction. Solid-state MAS <sup>29</sup>Si NMR measurements of the isolated powder revealed a chemical shift of  $-103.5 \text{ ppm}$ , well in line with a polymeric  $[\mathbf{1}]_n$ .<sup>[19]</sup> Although  $[\mathbf{1}]_n$  is insoluble in common non-coordinating organic solvents, it rapidly dissolved upon adding the respective  $\text{PPh}_4$ - or  $\text{NBu}_4$ -salts or by reaction with potassium or lithium salts in the presence of suitable crown ethers (Scheme 1b, for details, see Supporting Information). Hence, polymeric  $[\mathbf{1}]_n$  acts as a source of “free” **1** by Si–O metathesis depolymerization.

The  $\text{PPh}_4$  salts of the halide adducts  $[\text{Cl-}\mathbf{1}]^-$ ,  $[\text{Br-}\mathbf{1}]^-$  and  $[\text{I-}\mathbf{1}]^-$  exhibit <sup>29</sup>Si NMR chemical shifts along the electronegativity trend of the halides (Table 2, all values in  $\text{CD}_2\text{Cl}_2$ ). While the <sup>29</sup>Si NMR signal of the chloride adduct occurs at  $-90.4 \text{ ppm}$ ,<sup>[15b]</sup> the respective signals for the bromide and iodide adduct are upfield shifted to  $-96.0$  and  $-113.4 \text{ ppm}$ , respectively. Noteworthily, the fluoride adduct does not match this trend ( $-105.1 \text{ ppm}$ ). Hence, this order is similar to the shifts of neutral tetrahalidosilanes  $\text{SiX}_4$  ( $\text{X}=\text{Cl}>\text{Br}>\text{F}>\text{I}$ ).<sup>[20]</sup> Interestingly, the <sup>13</sup>C NMR chemical shifts of the *ipso*-carbon atom of the catechol ligand linearly increase from  $144.9$  for  $[\text{I-}\mathbf{1}]^-$  to  $145.8 \text{ ppm}$  for the respective fluoride adduct (see Table 2, col 4).

The thiocyanate adduct exhibits a broad signal at  $\delta(^{29}\text{Si})=-110.6 \text{ ppm}$ . Based on the significant enthalpy difference of both coordination isomers ( $\Delta\Delta H_{\text{sol}}=66.2 \text{ kJ mol}^{-1}$ , Ta-



**Scheme 1.** a) Synthesis of polymeric  $[1]_n$ , as a source of “donor free” **1** and b) synthesis of anionic silicates considered in this study.

**Table 2:** Experimental  $^{29}\text{Si}$  and  $^{13}\text{C}$  NMR chemical shifts [ppm] of the adducts  $[\text{X-}1]^-$  in  $\text{CD}_2\text{Cl}_2$ , and DFT computed values (SO-ZORA-PBE0/TZ2P).

$[\text{X-}1]^-$	$\delta(^{29}\text{Si})_{\text{exp}}$	$\delta(^{29}\text{Si})_{\text{calc}}$	$\delta(^{13}\text{C})^{[a]}$
$\text{F}^{[15a]}$	-105.1	-102.2	145.8
$\text{Cl}^{[15b]}$	-90.4	-91.7	145.5
$\text{Br}$	-96.0	-89.2	145.2
$\text{I}$	-113.4	-106.6	144.9
$\text{N}_3^{[b]}$	-99.9	-96.7	146.3
$\text{HCO}_2^{[c]}$	-107.9	-100.6 (-127.7)	145.7
$\text{H}_3\text{CCO}_2^{[b,c]}$	-107.6	-103.1 (-132.6)	146.9
$-\text{NCS}$	-110.6	-107.6 [-81.3]	145.5
$[-\text{SCN}]$			
$\text{TfO}^{[d]}$	-105.9	-99.9 (-134.5)	145.2
$[\text{1-SO}_4\text{-}1]^{2-}$	-108.0	-103.9	149.9

<sup>[a]</sup> ipso-carbon of the catechol ligand, <sup>[b]</sup> measured in  $\text{o-DCB}$ . <sup>[c]</sup>  $\kappa^2$ -mode in parentheses.

ble 1), a  $\kappa\text{-N}/\kappa\text{-S}$ -equilibrium appeared unlikely as a cause for signal broadening. Alternatively, a reversible interaction of the terminal sulfur with another unit of  $[\text{SCN-}1]^-$  occurs. However, only the N-coordinated isomer  $[\text{SCN-}1]^-$  was characterized by single-crystal XRD (see structural discussion below). The formate and acetate adducts  $[\text{K@18-c-6}][\text{HCO}_2\text{-}1]$  and  $[\text{K@18-c-6}][\text{H}_3\text{CCO}_2\text{-}1]$  exhibit similar

$^{29}\text{Si}$  NMR chemical shifts ( $\delta(^{29}\text{Si}) = -107.9$  and  $-107.6$  ppm). Compared to  $[\text{K@18-c-6}][\text{HCO}_2]$ , the  $^{13}\text{C}$  NMR chemical shift of the carboxyl carbon signal in the adduct is upfield shifted by 7.2 ppm. This apparent “shielding” might originate from the ring current anisotropy of the catechol  $\pi$ -system located near the anion. In contrast, the literature known adduct  $[\text{H}_2\text{TMP}][\text{HCO}_2\text{-B}(\text{C}_6\text{F}_5)_3]$  exhibits a slight downfield shift of the carboxylic  $^{13}\text{C}$  NMR signal ( $\Delta\delta(^{13}\text{C}) = +1.7$ ).<sup>[21]</sup> The effect of **1** can also be observed at the formate proton, upfield shifted by  $\Delta\delta(^1\text{H}) = -0.49$  ppm in the  $^1\text{H}$  NMR spectrum of  $[\text{K@18-c-6}][\text{HCO}_2\text{-}1]$ . Although it was impossible to resolve the signal for the quaternary carboxyl carbon in the  $^{13}\text{C}$  NMR of the acetate adduct  $[\text{AcO-}1]^-$ , an upfield shift of  $\Delta\delta(^{13}\text{C}) = -4.5$  ppm of the methyl group indicates a similar effect in this compound.

To support the interpretation of the experimental spectra, the  $^{29}\text{Si}$  NMR chemical shifts for the proposed adducts were computed by density functional theory (Table 2, col 2 and Supporting Information section 3d). Generally, these values match well with the experimental data, allowing to assign the  $\kappa\text{-N}$  isomer for the thiocyanate adduct and a  $\kappa^1$ -binding mode for formate and acetate in solution. Although the  $\kappa^2$ -bound acetate was computed more stable (see Table 1), entropic effects, explicit solvation, or cation interactions appear to stabilize the  $\kappa^1$ -isomer.

The weakly coordinating triflate anion also forms stable adducts  $[\text{TfO-}1]^-$ , with a  $^{29}\text{Si}$  NMR chemical shift of  $-105.9$  ppm. As for the carboxylates, **1** has a shielding effect on the nuclei adjacent to the coordinating oxygen atom. This leads to slightly upfield shifted signals for the  $\text{CF}_3$  group of  $[\text{K@18-c-6}][\text{TfO-}1]$  in comparison to  $[\text{K@18-c-6}][\text{OTf}]$ , ( $\Delta\delta(^{13}\text{C}) = -1.8$  ppm). Similar upfield shifts can be found, e.g., in the covalent  $\text{Ph}_3\text{SiOTf}$ , which can be regarded as an adduct of a triphenylsilyl cation and a triflate anion ( $\Delta\delta(^{13}\text{C}) = -2.5$  ppm).<sup>[22]</sup> This latter comparison illustrates that the binding of a strong Lewis acid to an anion not necessarily needs to cause an NMR deshielding, but might be governed by anisotropy effects.

A sulfate adduct formed by the reaction of  $\text{K}_2\text{SO}_4$  and  $1\text{-}( \text{sulfolane})_2$  in presence of dibenzo-18-crown-6 (*db-18-c-6*). While the  $^{29}\text{Si}$  NMR chemical shift is comparable to the other pentavalent silicon species ( $\delta(^{29}\text{Si}) = -108.0$  ppm), the  $^{13}\text{C}$  NMR signals of the catechol atoms were downfield shifted, indicating a peculiarity for this compound. Indeed, this difference was disclosed by SCXRD (see below), revealing a sulfate-dianion bridging two units of **1**. Hence, the observed NMR spectroscopic difference can be attributed to neighboring aromatic ring systems, which are absent in the 1:1 adducts. This 1:2 type of binding occurred irrespective of the applied stoichiometry. Similar observations were made for the reaction of  $[1]_n$  and  $[\text{NBu}_4]_2[\text{SO}_4]$ .

The perturbation effect of **1** on anions was further probed by ATR-FTIR spectroscopy of the reaction solutions. Note that those values can be affected by the influence of vibrational coupling. The NN-stretching mode in the azide adduct  $[\text{NBu}_4][\text{N}_3\text{-}1]$  ( $\nu = 2137 \text{ cm}^{-1}$ ) is blue-shifted by  $137 \text{ cm}^{-1}$  compared to free tetrabutylammonium azide.<sup>[23]</sup> A less distinct blue shift was observed in the literature known adduct  $[\text{C}_{30}\text{H}_{48}\text{N}_4\text{Sb}_2][\text{N}_3\text{-B}(\text{C}_6\text{F}_5)_3]$  ( $\nu = 2123 \text{ cm}^{-1}$ ),<sup>[24]</sup> and

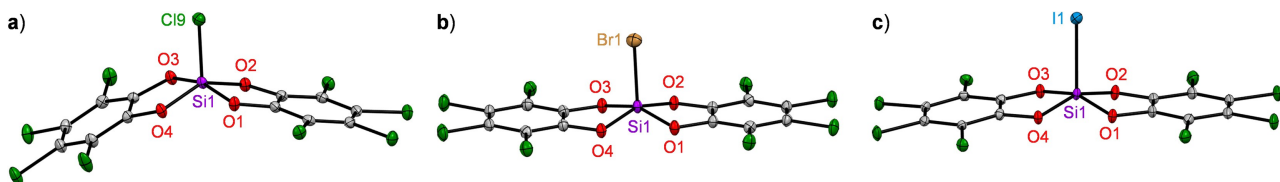


**Figure 2.** Molecular structures of a)  $[PPh_4][Cl\text{-}1]$ , b)  $[PPh_4][Br\text{-}1]$  and c)  $[PPh_4][I\text{-}1]$  (only one of two molecules is shown). Cations, cocrystallized solvent molecules and hydrogen atoms are omitted for clarity. Displacement ellipsoids are drawn with a probability of 50%. Selected structural parameters see Table 3.

even in TMS-N<sub>3</sub> ( $\nu=2132\text{ cm}^{-1}$ ).<sup>[16b]</sup> A similar effect can be observed in the IR spectrum of  $[PPh_4][SCN\text{-}1]$ , in which the band for the CN-stretching mode ( $\nu=2081\text{ cm}^{-1}$ ) is blue-shifted by  $29\text{ cm}^{-1}$  compared to  $[PPh_4][SCN]$ . This blue shift is more pronounced than in the covalently bound TMS-NCS ( $\nu=2052\text{ cm}^{-1}$ ), but less than in the adduct  $[K@18\text{-c-6}][SCN\text{-}B(C_6F_5)_3]$  ( $\nu=2146\text{ cm}^{-1}$ ).<sup>[16b,25]</sup> The signal for the CO carbonyl/carboxyl stretching mode in  $[K@18\text{-c-6}][HCO_2\text{-}1]$  ( $\nu=1720\text{ cm}^{-1}$ ) is strongly blue-shifted by  $122\text{ cm}^{-1}$  compared to potassium formate. Like in the case of the azide adduct, this blue shift is more distinct than in the adduct  $[H_2TMP][HCO_2\text{-}B(C_6F_5)_3]$  ( $\nu=1641\text{ cm}^{-1}$ ).<sup>[21]</sup>

Molecular structures for all adducts were obtained by single-crystal X-ray diffraction analysis. Within the halogen series, the expected trend in the Si–X bond length is observed (Figure 2 and Table 3, col. 3). The silicon centers for the heavier halides (Br, I) are coordinated almost ideally square pyramidal (topology parameter<sup>[26]</sup> TP = 0.002–0.053, for *sp* TP = 0), whereas for the chlorido (TP = 0.267) deformation toward the trigonal-bipyramidal (*tbp*) structure is noted. This trend only loosely conforms to the influence of apicophilicity for the respective halides.<sup>[27]</sup> Note that bromide and iodide adducts of tris(pentafluorophenyl)borane are unknown.

The adduct of the azide-anion  $[NBu_4][N_3\text{-}1]$  exhibits a TP = 0.519, ranging between *sp* and *tbp* (Figure 3a). The Si1–N1 bond is short ( $1.7659(14)\text{ \AA}$ ) compared to neutral, pentacoordinate silicon(IV)-*pseudo*-halido complexes (e.g., Tackes  $[ONO]PhSiN_3$ :  $1.8378(12)\text{ \AA}$ ,  $[ONO]$  = tridentate, dianionic O,N,O-ligand).<sup>[28]</sup> The deviation of the N1–N2

bond lengths from “free” azide ( $1.17\text{ \AA}$  in  $NaN_3$ )<sup>[29]</sup> is significantly stronger in  $[N_3\text{-}1]^-$  ( $N1\text{-}N2 = 1.2303(19)\text{ \AA}$ ) as compared to  $[N_3\text{-}B(C_6F_5)_3]^-$  ( $1.206(4)\text{ \AA}$ ). An  $N_3$ -bridged dimeric compound, as in the azido diborate anion  $[(C_6F_5)_3B\text{-}N_3\text{-}B(C_6F_5)_3]^-$ ,<sup>[30]</sup> was not observed with **1**. Instead, the bis-azide-dianion  $[(N_3)_2\text{-}1]^{2-}$  could be obtained (Figure 3b). It is a rare example of a *cis*-configured bis-adduct of bis(perchlorocatecholato)silane.

Compound  $[NBu_4][SCN\text{-}1]$  displays a pentacoordinate environment around the silicon center between *sp* and *tbp* (Figure 3c, TP = 0.430). The respective neutral SCN-SiPh-[ONO] compound or a silatrane isothiocyanate complex SCN-Si(N(CH<sub>2</sub>CH<sub>2</sub>O)<sub>3</sub>) both exhibit significantly longer Si–N bonds ( $1.8470(12)$  and  $1.800(3)\text{ \AA}$ ).<sup>[28,31]</sup> In the corresponding  $[SCN\text{-}B(C_6F_5)_3]^-$  adduct,<sup>[25]</sup> the N–C bond ( $1.180(3)$  vs.  $1.181(6)\text{ \AA}$  in  $[SCN\text{-}1]^-$ ) and the C–S bond ( $1.598(2)$  vs.  $1.582(5)\text{ \AA}$  in  $[SCN\text{-}1]^-$ ) are again more disturbed in the complex with **1**, compared to “free” SCN<sup>−</sup> ( $1.128(4)$  and  $1.675(3)\text{ \AA}$  in  $PPh_4SCN$ ).<sup>[32]</sup> Noteworthy, the isothiocyanate adduct with  $PPh_4^+$  as the cation displays different structural parameters, potentially caused by interactions with the cation (see section 3a in the Supporting Information).

In  $[HCO_2\text{-}1]^-$ , formate binds in a  $\kappa^1$ -fashion with the Si1–O5 bond length of  $1.6928(15)\text{ \AA}$  (Figure 4a). The O5–C13 bond length of  $1.322(2)\text{ \AA}$  is considerably elongated, and the O6–C13 bond of  $1.196(3)\text{ \AA}$  is shortened compared to “free” formate ( $1.2400(15)$  and  $1.2429(14)\text{ \AA}$  in  $[H_2NCy_2][HCO_2]$ ).<sup>[33]</sup>

Again,  $[Na@15\text{-c-5}][HCO_2\text{-}B(C_6F_5)_3]$  exhibits a less disturbed C=O ( $1.222(4)\text{ \AA}$ ) and C–O bond ( $1.302(3)\text{ \AA}$ ).<sup>[21,34]</sup> In the acetate adduct  $[H_3CCO_2\text{-}1]^-$ , the Si1–O1 bond lengths are almost equal ( $1.690(3)$  as in  $[HCO_2\text{-}1]^-$  (Figure 4b)). The C13–O5 bond within the anion is elongated ( $1.341(5)\text{ \AA}$ ), and the C13–O6 bond is shortened ( $1.215(5)\text{ \AA}$ ) compared to the acetate in  $[NBu_4][H_3CCO_2]$  ( $1.2535(16)$  and  $1.2474(17)\text{ \AA}$ ).<sup>[35]</sup> Again, the degree of structural perturbation is more pronounced than in the respective adduct with  $B(C_6F_5)_3$ .<sup>[36]</sup>

Molecular structures of  $[TfO\text{-}1]^-$  were obtained within different salts. Interestingly, the structural features do not strongly depend on the type of counteraction (for a discussion, see section 3b in the Supporting Information). Figure 4c shows the structure for  $[K@18\text{-c-6}][TfO\text{-}1]$ . All silicon coordination environments lie on the *sp* side (TP between 0.003 and 0.095), and the Si1–O5 bond lengths (O5 is the coordinating triflate-O-atom) are in between the range

**Table 3:** Topology parameters TP and selected bond lengths [ $\text{\AA}$ ] of anionic mono-adducts  $[X\text{-}1]^-$  and  $[1\text{-}SO_4\text{-}1]^{2-}$ .

$[X\text{-}1]^-$	TP	$d(\text{Si-X})$	$d(\text{Si-O}_{\text{cat},\text{av}})$
$F^{[15a]}$	0.047	1.6057(13)	1.7366(14)
$Cl^{[15b]}$	0.267	2.0867(8)	1.7371(15)
Br	0.002	2.2560(5)	1.7296(13)
I	0.027	2.5297(9)	1.735(2)
$N_3$	0.519	1.7659(14)	1.7370(11)
$[(N_3)_2\text{-}1]^{2-}$	–	1.883(11) 1.883(10)	1.7852(17)
$HCO_2$	0.362	1.6928(15)	1.7333(14)
$H_3CCO_2$	0.274	1.690(3)	1.742(3)
NCS	0.430	1.755(4)	1.732(3)
TFO <sup>[c]</sup>	0.029	1.740(17)	1.721(13)
$[1\text{-}SO_4\text{-}1]^{2-}$	0.004	1.702(3)	1.726(2)

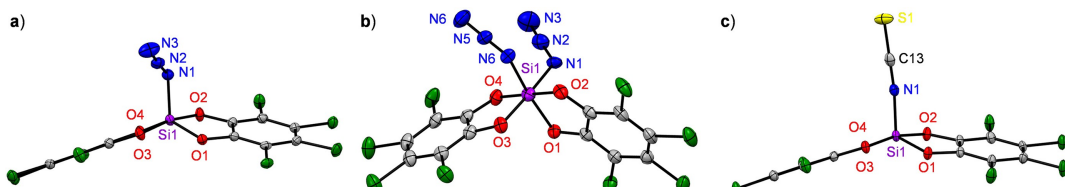


**Figure 3.** Molecular structures of a)  $[\text{NBu}_4]\text{[N}_3\text{-1]}$ , b)  $[\text{NBu}_4]_2\text{[(N}_3\text{)}_2\text{-1]}$  and c)  $[\text{NBu}_4]\text{[SCN-1]}$ . Cations and disorder are omitted for clarity. Displacement ellipsoids are drawn with a probability of 50%. Selected bond lengths [ $\text{\AA}$ ] and bond angles [ $^\circ$ ]: a) N1–N2 1.2303(19), N2–N3 1.118(2), N1–N2–N3 174.54(17), Si1–N1–N2 122.80(11), b) N1–N2 1.203(12), N2–N3 1.159(9), N1–N2–N3 176.5(17), Si1–N1–N2 123.5(12), N4–N5 1.206(11), N4–N6 1.146(7), N4–N5–N6 176.5(8), Si1–N4–N5 120.9(9) and c) N1–C13 1.181(6), C13–S1 1.582(5), N1–C13–S1 179.9(5), Si1–N1–C13 173.7(3); for TP, Si–X and Si–O<sub>cat,av</sub> see Table 3.

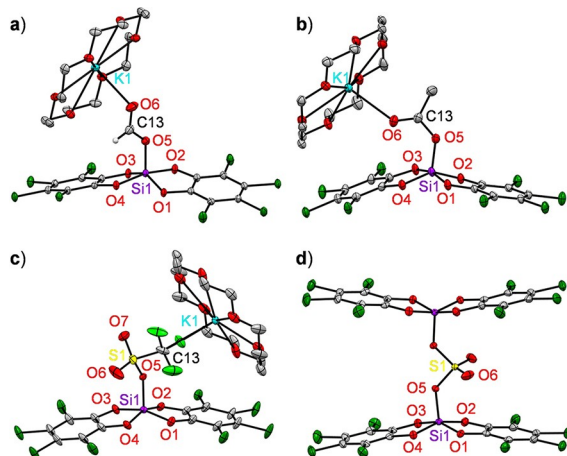


**Figure 4.** Molecular structures of a)  $[\text{K}@\text{18-c-6}]\text{[HCO}_2\text{-1]}$  and b)  $[\text{K}@\text{18-c-6}]\text{[H}_3\text{CCO}_2\text{-1]}$ , c)  $[\text{K}@\text{18-c-6}]\text{[TfO-1]}$  and d)  $[\text{NBu}_4]_2\text{[1-SO}_4\text{-1]}$ . Cocrystallized solvent molecules, disorder, hydrogen atoms (except the formic hydrogen), and the  $[\text{NBu}_4]$  cations in (d) are omitted for clarity. Displacement ellipsoids are drawn with a probability of 50%. Selected bond lengths [ $\text{\AA}$ ] and bond angles [ $^\circ$ ]: a) O5–C13 1.322(2), O6–C13 1.196(3), O5–C13–O6 123.0(2), b) O5–C13 1.341(5), O6–C13 1.215(5), O5–C13–O6 123.3(4), c) S1–O5 1.485(9), S1–O6 1.421(3), S1–O7 1.428(5), S1–C13 1.813(7) and d) S1–O5 1.536(2), S1–O6 1.414(3); for TP, Si–X and Si–O<sub>cat,av</sub> see Table 3.

of 1.731(4) and 1.766(3)  $\text{\AA}$ . To the best of our knowledge, no other structurally characterized anionic Lewis Acid-OTf adducts exist in the literature. The neutral compound tris(pentafluorophenyl)silyl triflate ( $\text{C}_6\text{F}_5\text{)}_3\text{Si(OTf)}$ ) exhibits a Si–O bond length of 1.663(2)  $\text{\AA}$ , which is considerably shorter than in the anionic adducts  $[\text{TfO-1}]^-$ .<sup>[37]</sup>

Compared to the free triflate, the S1–O5 bond is significantly longer in  $[\text{TfO-1}]^-$  (1.485(9)–1.515(3)  $\text{\AA}$ ) as compared to 1.440(5)  $\text{\AA}$  in  $\text{AgOTf}$ <sup>[38]</sup> or 1.440(3)  $\text{\AA}$  in  $[\text{BPh}_2\text{-}(\text{MesIm})_2]\text{[OTf]}$ .<sup>[39]</sup> Similar sulfur–oxygen bond elongations are observable in  $(\text{C}_6\text{F}_5\text{)}_3\text{Si(OTf)}$  (S1–O1 1.510(2), S1–O(2–3)<sub>av</sub> 1.433(3)  $\text{\AA}$ ).<sup>[37]</sup>

The reaction of  $[\mathbf{1}]_n$  and  $[\text{NBu}_4]_2\text{SO}_4$  yielded, irrespective of the applied stoichiometry, a dianionic 1:2 adduct  $[\mathbf{1}-\text{SO}_4\text{-1}]^{2-}$  (Figure 4d). The sulfate dianion bridges both Lewis acidic centers via its S1–O5 single bonds, whereas the other S1–O6 bonds remain uninvolved. To the best of our knowledge,  $[\mathbf{1}-\text{SO}_4\text{-1}]^{2-}$  represents a scarce example of a Lewis acid-sulfate adduct. A search in the CCDC revealed sulfates

generally to be part of extended ionic lattices.<sup>[40]</sup> Only one example of a main group Lewis acid, namely the clathrate  $\text{K}_2\text{[(SO}_4\text{)}_2\text{(AlMe}_3\text{)}_4]$ ,<sup>[41]</sup> and one transition metal-bound ( $\kappa^1\text{-SO}_4$ )-iron porphyrin complex are known.<sup>[42]</sup>

With this set of putative models for intermediates in Lewis base catalysis in hand (cf. Figure 1a), comparisons on structural and electronic perturbations, and thus, evaluating Gutmann's empirical rules, were possible. The averaged bond length to the catecholato ligands Si–O<sub>cat</sub> provides a metric parameter for the degree of "structural activation" (Rule 1). A Si–O<sub>cat</sub> bond elongation is noted for all adducts (Table 3, col 4) with reference to the "free" Lewis acid in the gas phase (1.644(1)  $\text{\AA}$ ),<sup>[19]</sup> but these values neither correlate with the Si–X bond lengths (Table 3, col 3, for computed trends, see Table S3.1) nor with ion affinity (Table 1). Interestingly, the acetate induces the most pronounced Si–O<sub>cat</sub> bond elongation. This fact might eventually be related to acetate's unusual activity in Lewis base catalysis.<sup>[3c,5]</sup> As a parameter for the "electronic activation" of silicon, that is, the increased electrophilicity at silicon upon Lewis base binding, natural charges were obtained from natural population analysis (PBE0/def2-TZVPP electron density, with/without CPCM solvation correction, Table S3.5). The silicon atoms in all adducts exhibit a significant positive polarization (+2.32 to +2.00). Hence, in line with previous findings, the situation at silicon does not correspond to *hypervalency* but is better described by the term *hypercoordination*.<sup>[43]</sup> Further, the positive charge at silicon was found largest for the fluorido (+2.32) and acetato (+2.30) adduct, which are among the most commonly employed Lewis bases for "initiation". However, compared to monomeric **1** (+2.38), the positive polarization diminishes in all adducts. This finding contradicts Gutmann's second empirical rule, but supports earlier high-level computations: an enhancement of positive polarization in silicon complexes is obtained only at the Hartree–Fock level of theory—but not with methods that consider electron correlation.<sup>[3c]</sup>

## Conclusion

Using bis(perchlorocatecholato)silane **1** as a binding platform, the structural chemistry of silicon is extended by the first bromido-, iodido-, formato-, acetato-, triflato- or

sulfato-silicates. Hence, the unequivocal observation of such adducts with weak bases substantiates their involvement in Lewis base-initiated silicon chemistry. Parameters derived from SCXRD and quantum chemical computations reveal the structural and electronic activation the anionic donors exert on **1** and allow for a reevaluation of Gutmann's empirical rules of donor-acceptor interactions (namely: 1) the shorter the donor-acceptor bond, the more pronounced the induced lengthening of the other peripheral bonds in the acceptor entity; 2) the positive polarization of the acceptor atom increases in the adducts).<sup>[4]</sup> Interestingly, the present data set does *not* support these rules. Besides, inspecting the structural and spectroscopic changes in the bound anions reveals that **1** induces polarization more substantial than the benchmark Lewis acid  $B(C_6F_5)_3$ . Hence, applications of **1**, e.g., to enable redox chemistry for substrates challenging to reduce, are indicated.<sup>[44]</sup> Further, given the role of anionic bis(catecholato)silicates in the photoredox catalytic formation of radicals, the herein presented salts might serve as precursors for synthetically valuable inorganic radicals.<sup>[45]</sup>

### Acknowledgements

We thank Prof. H.-J. Himmel for his constant support. This work was supported by Deutsche Forschungsgemeinschaft (grants GR 5007/2-1) and by Fonds der Chemischen Industrie. The authors acknowledge support by the state of Baden-Württemberg through bwHPC and the German Research Foundation (DFG) through grant no INST 40/575-1 FUGG (JUSTUS 2 cluster). D.H. is grateful to the Friedrich Ebert Foundation (FES) for a fellowship. Special thanks go to Dr. J. Graf for his help with solid-state NMR. Open Access funding enabled and organized by Projekt DEAL.

### Conflict of Interest

The authors declare no conflict of interest.

### Data Availability Statement

The data that support the findings of this study are available in the Supporting Information of this article.

**Keywords:** Anionic Silicates · Hypercoordination · Lewis Base Catalysis · Lewis Superacid · Silicon

[1] a) S. N. Tandura, M. G. Voronkov, N. V. Alekseev, *Structural Chemistry of Boron and Silicon*, Springer Berlin Heidelberg, Berlin, **1986**, pp. 99–189; b) D. Kost, I. Kalikhman, *Organic Silicon Compounds*, Wiley, Hoboken, **2009**; c) W. Levason, G. Reid, W. Zhang, *Coord. Chem. Rev.* **2011**, *255*, 1319–1341; d) J. Wagler, U. Böhme, E. Kroke in *Functional Molecular Silicon Compounds I: Regular Oxidation States* (Ed.: D. Scheschkewitz), Springer International Publishing, Cham, **2014**, pp. 29–

- 105; e) A. A. Nikolin, V. V. Negrebetsky, *Russ. Chem. Rev.* **2014**, *83*, 848.
- [2] a) C. Chuit, R. J. P. Corriu, C. Reye, J. C. Young, *Chem. Rev.* **1993**, *93*, 1371–1448; b) A. D. Dilman, S. L. Ioffe, *Chem. Rev.* **2003**, *103*, 733–772; c) S. Rendler, M. Oestreich, *Synthesis* **2005**, 1727–1747.
- [3] a) S. E. Denmark, T. Wynn, *J. Am. Chem. Soc.* **2001**, *123*, 6199–6200; b) S. E. Denmark, G. L. Beutner, T. Wynn, M. D. Eastgate, *J. Am. Chem. Soc.* **2005**, *127*, 3774–3789; c) S. E. Denmark, G. L. Beutner, *Angew. Chem. Int. Ed.* **2008**, *47*, 1560–1638; *Angew. Chem.* **2008**, *120*, 1584–1663; d) E. Vedejs, S. E. Denmark, *Lewis base catalysis in organic synthesis*, Wiley-VCH, Weinheim, **2016**.
- [4] a) V. Gutmann, *Coord. Chem. Rev.* **1975**, *15*, 207–237; b) V. Gutmann, *The donor-acceptor approach to molecular interactions*, Plenum Press, New York, **1978**.
- [5] G. L. Beutner, S. E. Denmark, *Angew. Chem. Int. Ed.* **2013**, *52*, 9086–9096; *Angew. Chem.* **2013**, *125*, 9256–9266.
- [6] a) K. Miura, T. Nakagawa, A. Hosomi, *J. Am. Chem. Soc.* **2002**, *124*, 536–537; b) N. Takashi, F. Hidehiko, N. Yuzo, M. Teruaki, *Bull. Chem. Soc. Jpn.* **2004**, *77*, 1555–1567; c) K. Yoshikazu, F. Hidehiko, M. Teruaki, *Chem. Lett.* **2005**, *34*, 614–615; d) K. Yoshikazu, F. Hidehiko, M. Teruaki, *Chem. Lett.* **2005**, *34*, 1134–1135; e) K. Yoshikazu, K. Nobuya, M. Teruaki, *Chem. Lett.* **2005**, *34*, 1508–1509.
- [7] a) D. Chen, C. Ni, Y. Zhao, X. Cai, X. Li, P. Xiao, J. Hu, *Angew. Chem. Int. Ed.* **2016**, *55*, 12632–12636; *Angew. Chem.* **2016**, *128*, 12822–12826; b) K. Kikushima, M. Grellier, M. Ohashi, S. Ogoshi, *Angew. Chem. Int. Ed.* **2017**, *56*, 16191–16196; *Angew. Chem.* **2017**, *129*, 16409–16414; c) W. B. Liu, D. P. Schuman, Y. F. Yang, A. A. Toutov, Y. Liang, H. F. T. Klare, N. Nesnas, M. Oestreich, D. G. Blackmond, S. C. Virgil, S. Banerjee, R. N. Zare, R. H. Grubbs, K. N. Houk, B. M. Stoltz, *J. Am. Chem. Soc.* **2017**, *139*, 6867–6879; d) A. A. Toutov, K. N. Betz, D. P. Schuman, W.-B. Liu, A. Fedorov, B. M. Stoltz, R. H. Grubbs, *J. Am. Chem. Soc.* **2017**, *139*, 1668–1674; e) C. P. Johnston, T. H. West, R. E. Dooley, M. Reid, A. B. Jones, E. J. King, A. G. Leach, G. C. Lloyd-Jones, *J. Am. Chem. Soc.* **2018**, *140*, 11112–11124; f) P. Asgari, Y. Hua, A. Bokka, C. Thiamsiri, W. Prasitwatcharakorn, A. Karedath, X. Chen, S. Sardar, K. Yum, G. Leem, B. S. Pierce, K. Nam, J. Gao, J. Jeon, *Nat. Catal.* **2019**, *2*, 164–173; g) A. García-Domínguez, T. H. West, J. J. Primozic, K. M. Grant, C. P. Johnston, G. G. Cumming, A. G. Leach, G. C. Lloyd-Jones, *J. Am. Chem. Soc.* **2020**, *142*, 14649–14663.
- [8] a) A. Corma, H. García, *Chem. Rev.* **2003**, *103*, 4307–4366; b) L. Greb, *Chem. Eur. J.* **2018**, *24*, 17881–17896.
- [9] N. Kano in *Organosilicon Compounds* (Ed.: V. Y. Lee), Academic Press, **2017**, pp. 645–716.
- [10] a) E. Bär, W. P. Fehlhammer, D. K. Breitinger, J. Mink, *Inorg. Chim. Acta* **1984**, *82*, L17–L19; b) M. Fritz, D. Rieger, E. Bär, G. Beck, J. Fuchs, G. Holzmann, W. P. Fehlhammer, *Inorg. Chim. Acta* **1992**, *198–200*, 513–526; c) J. Harloff, D. Michalik, S. Nier, A. Schulz, P. Stoer, A. Villinger, *Angew. Chem. Int. Ed.* **2019**, *58*, 5452–5456; *Angew. Chem.* **2019**, *131*, 5506–5511; d) Z. M. Smallwood, M. F. Davis, J. G. Hill, L. J. R. James, P. Portius, *Inorg. Chem.* **2019**, *58*, 4583–4591; e) J. Harloff, K. C. Laatz, S. Lerch, A. Schulz, P. Stoer, T. Strassner, A. Villinger, *Eur. J. Inorg. Chem.* **2020**, 2457–2464.
- [11] a) W. Heininger, R. Stucka, G. Nagorsen, *Z. Naturforsch. B* **1986**, *41*, 702–707; b) S. P. Narula, R. Shankar, M. Kumar, Meenu, *Inorg. Chem.* **1994**, *33*, 2716–2718; c) S. P. Narula, Meenu, R. D. Anand, J. K. Puri, R. Shankar, *Main Group Met. Chem.* **2000**, *23*, 405–408; d) P. Portius, M. Davis, *Dalton Trans.* **2010**, *39*, 527–532.
- [12] a) A. C. Filippou, P. Portius, G. Schnakenburg, *J. Am. Chem. Soc.* **2002**, *124*, 12396–12397; b) P. Portius, A. C. Filippou, G.

- Schnakenburg, M. Davis, K.-D. Wehrstedt, *Angew. Chem. Int. Ed.* **2010**, *49*, 8013–8016; *Angew. Chem.* **2010**, *122*, 8185–8189; c) W. P. Fehlhammer, W. Beck, *Z. Anorg. Allg. Chem.* **2013**, *639*, 1053–1082; d) P. Portius, M. Davis, *Dalton Trans.* **2016**, *45*, 17141–17152.
- [13] a) W. Heininger, K. Polborn, G. Nagorsen, *Z. Naturforsch. B* **1988**, *43*, 857–861; b) O. Seiler, R. Bertermann, N. Buggisch, C. Burschka, M. Penka, D. Tebbe, R. Tacke, *Z. Anorg. Allg. Chem.* **2003**, *629*, 1403–1411; c) O. Seiler, C. Burschka, K. Götz, M. Kaupp, S. Metz, R. Tacke, *Z. Anorg. Allg. Chem.* **2007**, *633*, 2667–2670; d) C. Logemann, T. Klüner, M. S. Wickleder, *Chem. Eur. J.* **2011**, *17*, 758–760; e) P. Portius, B. Peerless, M. Davis, R. Campbell, *Inorg. Chem.* **2016**, *55*, 8976–8984; f) Y. Wang, S. DeCarlo, L. Wang, L. Stevens, F. Chen, P. Zavalij, B. Eichhorn, *Inorg. Chem.* **2019**, *58*, 8915–8917; g) S. Arlt, K. Bläsing, J. Harloff, K. C. Laatz, D. Michalik, S. Nier, A. Schulz, P. Stoer, A. Stoffers, A. Villinger, *ChemistryOpen* **2021**, *10*, 62–71; h) I. Georg, M. Bolte, M. Wagner, H.-W. Lerner, *Z. Naturforsch. B* **2021**, *76*, 335–339.
- [14] a) S. Steinhauer, T. Böttcher, N. Schwarze, B. Neumann, H.-G. Stammmer, B. Hoge, *Angew. Chem. Int. Ed.* **2014**, *53*, 13269–13272; *Angew. Chem.* **2014**, *126*, 13485–13488; b) J. Tillmann, L. Meyer, J. I. Schweizer, M. Bolte, H.-W. Lerner, M. Wagner, M. C. Holthausen, *Chem. Eur. J.* **2014**, *20*, 9234–9239.
- [15] a) R. Maskey, M. Schädler, C. Legler, L. Greb, *Angew. Chem. Int. Ed.* **2018**, *57*, 1717–1720; *Angew. Chem.* **2018**, *130*, 1733–1736; b) D. Hartmann, M. Schädler, L. Greb, *Chem. Sci.* **2019**, *10*, 7379–7388.
- [16] a) M. Lehmann, A. Schulz, A. Villinger, *Angew. Chem. Int. Ed.* **2009**, *48*, 7444–7447; *Angew. Chem.* **2009**, *121*, 7580–7583; b) A. Schulz, A. Villinger, *Chem. Eur. J.* **2010**, *16*, 7276–7281.
- [17] Deposition Numbers 2143056, 2130747, 2130729, 2130730, 2130731, 2132184, 2130732, 2130733, 2130738, 2143058, 2130734, 2130735, 2130737, 2130736 and 2156191 contains the supplementary crystallographic data for this paper. These data are provided free of charge by the joint Cambridge Crystallographic Data Centre and Fachinformationszentrum Karlsruhe Access Structures service.
- [18] C. Laurence, J.-F. Gal, *Lewis Basicity and Affinity Scales*, Wiley, Hoboken, **2009**, pp i–xv.
- [19] D. Hartmann, T. Thorwart, R. Müller, J. Thusek, J. Schwabedissen, A. Mix, J. H. Lamm, B. Neumann, N. W. Mitzel, L. Greb, *J. Am. Chem. Soc.* **2021**, *143*, 18784–18793.
- [20] B. Wrackmeyer in *Annual Reports on NMR Spectroscopy*, Vol. 57 (Ed.: G. A. Webb), Academic Press, New York, **2006**, pp. 1–49.
- [21] A. E. Ashley, A. L. Thompson, D. O'Hare, *Angew. Chem. Int. Ed.* **2009**, *48*, 9839–9843; *Angew. Chem.* **2009**, *121*, 10023–10027.
- [22] A. Asadi, A. G. Avent, C. Eaborn, M. S. Hill, P. B. Hitchcock, M. M. Meehan, J. D. Smith, *Organometallics* **2002**, *21*, 2183–2188.
- [23] A. J. Pearson, M. N. I. Khan, J. C. Clardy, C. H. He, *J. Am. Chem. Soc.* **1985**, *107*, 2748–2757.
- [24] M. Lehmann, A. Schulz, A. Villinger, *Eur. J. Inorg. Chem.* **2012**, 822–832.
- [25] I. C. Vei, S. I. Pascu, M. L. H. Green, J. C. Green, R. E. Schilling, G. D. W. Anderson, L. H. Rees, *Dalton Trans.* **2003**, 2550–2557.
- [26] E. P. A. Couzijn, J. C. Slootweg, A. W. Ehlers, K. Lammertsma, *J. Am. Chem. Soc.* **2010**, *132*, 18127–18140.
- [27] R. R. Holmes, *Acc. Chem. Res.* **1979**, *12*, 257–265.
- [28] J. Weiβ, B. Theis, S. Metz, C. Burschka, C. Fonseca Guerra, F. M. Bickelhaupt, R. Tacke, *Eur. J. Inorg. Chem.* **2012**, 3216–3228.
- [29] S. B. Hendricks, L. Pauling, *J. Am. Chem. Soc.* **1925**, *47*, 2904–2920.
- [30] M. F. Silva Valverde, E. Theuerbergarten, T. Bannenberg, M. Freytag, P. G. Jones, M. Tamm, *Dalton Trans.* **2015**, *44*, 9400–9408.
- [31] S. P. Narula, R. Shankar, M. Kumar, R. K. Chadha, C. Janaik, *Inorg. Chem.* **1997**, *36*, 1268–1273.
- [32] S. Nuzzo, B. Twamley, J. A. Platts, R. J. Baker, *Chem. Commun.* **2016**, *52*, 13296–13298.
- [33] J. A. Odendaal, J. C. Bruce, K. R. Koch, D. A. Haynes, *CrystEngComm* **2020**, *22*, 7399–7406.
- [34] a) S. D. Tran, T. A. Tronic, W. Kaminsky, D. Michael Heinekey, J. M. Mayer, *Inorg. Chim. Acta* **2011**, *369*, 126–132; b) T. Voss, T. Mahdi, E. Otten, R. Fröhlich, G. Kehr, D. W. Stephan, G. Erker, *Organometallics* **2012**, *31*, 2367–2378; c) R. Kather, E. Lork, M. Vogt, J. Beckmann, *Z. Anorg. Allg. Chem.* **2017**, *643*, 636–641.
- [35] J. Hurmäläinen, M. A. Land, K. N. Robertson, C. J. Roberts, I. S. Morgan, H. M. Tuononen, J. A. Clyburne, *Angew. Chem. Int. Ed.* **2015**, *54*, 7484–7487; *Angew. Chem.* **2015**, *127*, 7592–7595.
- [36] S. Mitu, M. C. Baird, *Can. J. Chem.* **2006**, *84*, 225–232.
- [37] V. V. Levin, A. D. Dilman, P. A. Belyakov, A. A. Korlyukov, M. I. Struchkova, V. A. Tartakovskiy, *Eur. J. Org. Chem.* **2004**, 5141–5148.
- [38] W. Grochala, M. K. Cyranski, M. Derzsi, T. Michalowski, P. J. Malinowski, Z. Mazej, D. Kurzydlowski, W. Kozminski, A. Budzianowski, P. J. Leszczynski, *Dalton Trans.* **2012**, *41*, 2034–2047.
- [39] A. Kouton, Y. Gao, V. Carta, *Acta Crystallogr. Sect. E* **2020**, *76*, 673–676.
- [40] a) E. Coronado, S. Curreli, C. Gimenez-Saiz, C. J. Gomez-Garcia, A. Alberola, E. Canadell, *Inorg. Chem.* **2009**, *48*, 11314–11324; b) A. Yokoyama, T. Kojima, S. Fukuzumi, *Dalton Trans.* **2011**, *40*, 6445–6450; c) K. Kozma, M. Wang, P. I. Molina, N. P. Martin, Z. Feng, M. Nyman, *Dalton Trans.* **2019**, *48*, 11086–11093.
- [41] R. D. Rogers, J. L. Atwood, *Organometallics* **1984**, *3*, 271–274.
- [42] W. R. Scheidt, Y. J. Lee, M. G. Finnegan, *Inorg. Chem.* **1988**, *27*, 4725–4730.
- [43] N. Kocher, J. Henn, B. Gostevskii, D. Kost, I. Kalikhman, B. Engels, D. Stalke, *J. Am. Chem. Soc.* **2004**, *126*, 5563–5568.
- [44] a) R. Maskey, C. Bendel, J. Malzacher, L. Greb, *Chem. Eur. J.* **2020**, *26*, 17386–17389; b) V. Hosseiniinasab, A. C. McQuilken, A. G. Bakhoda, J. A. Bertke, Q. K. Timerghazin, T. H. Warren, *Angew. Chem. Int. Ed.* **2020**, *59*, 10854–10858; *Angew. Chem.* **2020**, *132*, 10946–10950.
- [45] a) V. Corcé, L.-M. Chamoreau, E. Derat, J.-P. Goddard, C. Ollivier, L. Fensterbank, *Angew. Chem. Int. Ed.* **2015**, *54*, 11414–11418; *Angew. Chem.* **2015**, *127*, 11576–11580; b) M. Jouffroy, D. N. Primer, G. A. Molander, *J. Am. Chem. Soc.* **2016**, *138*, 475–478; c) E. Levernier, K. Jaouadi, H.-R. Zhang, V. Corcé, A. Bernard, G. Gontard, C. Troufflard, L. Grimaud, E. Derat, C. Ollivier, L. Fensterbank, *Chem. Eur. J.* **2021**, *27*, 8782–8790.

Manuscript received: March 16, 2022

Accepted manuscript online: April 19, 2022

Version of record online: May 5, 2022